

# 25 Meter Millimeter Wave Telescope Memo #101

NATIONAL RADIO ASTRONOMY OBSERVATORY  
Charlottesville, Virginia

November 22, 1977

## MEMORANDUM

TO: 25-m Design Group  
FROM: W-Y. Wong  
SUBJECT: The Current Status of 25-m Back-Up Structure Design

This memo is written for the occasion of the 30-m design work shop meeting in Bonn, Germany on November 29th and 30th, 1977. I am to report the NRAO efforts on the design of the elevation structure. The elevation structure has been modified since the 1976 design. The changes were relatively minor and with a few cycles in the homology program, a good solution is again obtained. The new version has a large vertex cabin, big enough to have four receivers installed as a cluster (Figure 5). The vertex cabin also has a larger load capacity than the previous version. The cabin now is completely disconnected with the elevation shaft, so that the variation of loading in the cabin will not affect the deflection of the shaft. The cabin is located entirely below the surface, with space at the vertex area provided for the reference plates while the surface is being measured. The receivers are to be lowered from the front opening, when the telescope is in stow position.

Some latest development on the surface plate studies are also being described. I understand that the search for better surface plates is one of our main concerns.

Figure 4 describes the detail procedure for the analysis of the back-up structure in a flow chart form. The dashed outline denotes the planned steps to be taken in the future.

#### SURFACE PLATE

Presently we are proposing to use cast aluminum machined surface plates for the 25-m telescope. However, we are still active in searching other approaches for more accurate, lighter or even cheaper surfaces. We had two cast aluminum plates of two different alloys made in 1976. These two plates had already shown that the industry can machine the surface to an rms error of about .040 mm or less in a mass production fashion.

The plate weighs  $20 \text{ kg/m}^2$ . Outside dimensions measured about .7 m by 1.5 m. The thickness of the surface skin is machined to 3.2 mm. The depth of the stiffening rib system is 111 mm.

The general manufacturing procedure is as follows: First the aluminum is sand casted, then it is checked by obtaining radiographs for defects. The cast blank is heat-treated and stress released. Then it is placed in the N/C mill, and the first cut will machine the surface to about 1.5 mm to its theoretical surface. The plate is taken away from the machine and placed in the oven for stress release for 4 hours at about 350° F. The second machining procedure with the N/C mill will achieve the final surface. A N/C milling-machine with an accuracy of  $\pm .013 \text{ mm}$ , and repeatable to  $\pm .008 \text{ mm}$  is available, at a cost of about \$80,000. It is considered possible to machine a specimen to a tolerance within .025 mm.

We have tried two different types of aluminum alloys: A356 and Precedent 71. The later is a proprietary product, twice as expensive, supposed more stable in dimension and easier in machining. The experience of the manufacturer indicates no appreciable difference in machinability. Dimensional stability is difficult to check. The Precedent 71 A - T5 is claimed to be stable to within .025 mm, Precedent 71A - T52 within 0.0003 mm. Since the dimensional stability is a function of stress, and since there will be no appreciable loading on the surface plates, it seems there is no need for such a concern.

The gravity and thermal effects on the surface plate were resolved by structural analysis, using finite element method (709 nodes, 540 plate elements, 229 beam elements). The gravity effect, when the plate is supported horizontally by 4 corners, showed a deviation from the average:

$$\text{Gravity: rms } (\Delta Z - \overline{\Delta Z}) = .007 \text{ mm} \quad (1)$$

and the thermal deformation showed:

$$\text{Thermal: rms } (\Delta Z) = .049 \text{ mm/C}^\circ \quad (2)$$

based on the depth of the panel equals 111 mm, and the thermal gradient normal to the surface.

Meanwhile, the in-house effort in evaluating the surface plate involved the measurement of surface contours and temperature measurements on the plates in a radome environment. The surface measurements are accomplished by using an optical method, including a level (Wild N3) and a vertical rod. The plate was placed horizontal with a grid system laid out on the surface. The readings of the rod over each point are then

compared with the theoretical results. The estimated measuring error of this method is about .020 mm rms. The measurements\* of these two plates including the measurement error showed a result of:

$$\begin{aligned} \text{Surface error: rms } (\Delta Z - \overline{\Delta Z}) = & .044 \text{ mm (plate \#1)} \\ & .037 \text{ mm (plate \#2)} \end{aligned} \quad (3)$$

The temperature measurements are taken place in a tent of ESSCO's radome material ESSCOLAM X-106-3. The results showed that 1) the temperature difference between the outside and inside of the dome is always small; 2) the temperature difference between the inside air and the skin is small; and 3) the temperature difference between the skin and the ribs are

$$\begin{array}{llll} \text{day} & (0700 - 1800) & \text{rms } \Delta T = & 0.29^\circ\text{C} \\ \text{night} & (1900 - 0600) & \text{rms } \Delta T = & 0.19^\circ\text{C} \end{array} \quad (4)$$

We also investigated a plate from ESSCO, originally built for the University of Massachusetts telescope. Their design involved an aluminum frame work, epoxyed to a thin aluminum sheet which was held against an accurate mold by suction. The aluminum sheet is slotted at some intervals along the edge to reduce the internal stress due to the double curvature needed for forming. The NRAO measurements of this surface plate showed an error of .096 mm rms; this was subsequently verified by ESSCO with a result of 0.084 mm rms. According to ESSCO, this error can be reduced by further research and development.

---

\* The BTL-7m offset antenna also has plates of similar kind. Out of 21 measured samples, the worst plate has an error of .045 mm rms, the best has an error of .020 mm rms, and average of .035 mm rms. The repeatability of the measuring machine is .003 mm.

There is no decision if the surface should be painted. So far, investigations have shown that while paint reduced the thermal deformation during the day time by a factor of 5, it makes it worse by 40% during the night. It is because the paint is white in the visible, thus reducing the heat absorption from the sun, and is black in the far infrared, thus increasing its radiative cooling. Another concern is that the thickness of paint might not be uniform, adding an error to the measurement of surface. This problem might be solved by using ultra-sonic devices, or simply leaving some small areas unpainted. Also studies by the German 30-m telescope design group showed that reflective paints start to absorb at 150 GHz and above.

#### THERMAL DEFORMATION OF THE BACK-UP STRUCTURE

1. Temperature data - Two kinds of temperature data are required for the study of the thermal effects on the structure: temperature difference ( $\Delta T$ ) over the structure and the time derivative of ambient air temperature ( $\dot{T}$ ). These quantities should be measured, preferably on existing radio telescopes protected by radome or similar covering materials. This is specially true for the  $\Delta T$  curve which depends on cloud conditions, type of radome material, type of air handling system and so on. More efforts to get representative temperature data are planned in the future.

The  $\Delta T$  curve used in the analysis is derived from data of various sources. It was summarized by S. von Hoerner during the 65-m design. In addition, some data from the 36-ft. telescope in Tucson and the 13.7-m telescope in Brasil are also available. The

Tucson data were taken with the astrodome opened and the telescope was pointing close to zenith position, and also with good weather. The Brazilian data were taken in a radome, with a heater and a fan turned on in order to maintain a higher inside air temperature, intending to get rid of the condensation problem on the inside wall of the radome. Unfortunately all thermistors were not in good thermal contact with the metal of the telescope. The temperature difference within the dome might be misleading. However, this data offered information for the  $\dot{T}$  curve.

The absolute values of  $\Delta T$  curve used in the analysis implies two different kinds of operation modes. During the evening, the preliminary investigation indicated that temperature difference over the entire structure in the vertical direction is about  $2^{\circ}\text{C}$ . During the day time, when the astro-dome door is in closed position, and when the air circulating system is turned on, a temperature difference in the vertical direction can be maintained to within  $3^{\circ}\text{C}$  (Figure 1).

The  $\dot{T}$  curve, on the other hand, is considered quite reliable. Data collected from various sources showed good agreement except the time of occurrence of peak values, which are dependent on the season of the year. (Figure 1)

## 2. Deformation due to $1^{\circ}\text{C}$ Temperature Differences on the Structure -

Idealized thermal gradients with a difference of  $1^{\circ}\text{C}$  ( $\Delta T$ ) between two furthest points on the structure was applied as

thermal loadings. Two separate cases were considered in the analysis: that  $\Delta T$  on the structure lies along the telescope axis (Z direction -  $\Delta T_Z$ ) or across the aperture (Y direction -  $\Delta T_Y$ ). Each case was studied twice in the best fitting process in order to compare the focal adjustment effect on the surface accuracy. First study was to force the focal adjustment to zero, and the second study was to allow a focal adjustment. For example, the surface error in the  $\Delta T_Z$  case is .016 mm/C° without a focal adjustment, and became .001 mm/C° when the focal length is free to change. The sign conventions are shown in Figure 2 and the detail results of the best fit paraboloids are shown in Table 2.

TABLE 1

Influence of Thermal Gradient on the Back-up Structure With and Without Focal Adjustment

Loading	Best fit rms Surface error (mm)	dx	dy	dz	$\phi_x$	$\phi_y$	$\Delta F$
$\Delta T_Z = 1^\circ\text{C}$	.016	0.	0.	-.007	0.	0.	Forced to 0
	.001	0.	0.	+.017	0.	0.	+.151 mm
$\Delta T_Y = 1^\circ\text{C}$	.000	0.	-.022	0.	$-9 \times 10^{-7}$	0.	Forced to 0
	.000	0.	-.022	0.	$-9 \times 10^{-7}$	0.	0.

dx,dy,dz: Amount of shift of the best fit paraboloid vertex in x,y and z directions. Unit in mm.

$\phi_x, \phi_y$  : Amount of rotation of the best fit paraboloid about the X and Y axis. Unit in radian.

$\Delta F$  : required focal adjustment of the best fit paraboloid. Unit in mm.

These results are based on the idealized loading conditions. These analyses showed a focal adjustment with a temperature difference along the Z-axis will have an improvement on surface error by a factor of 16, which might be too optimistic. On the other hand, realistic temperature load is hard to simulate. Based on the past experience with the 36-ft. telescope in Tucson, vertical temperature gradient and focal adjustment are correlated, and a factor of 4 improvement was achieved<sup>\*</sup>. Hence a more realistic value was adopted, that the surface error of the telescope due to a one degree difference in vertical direction is:

$$\text{rms } (\Delta Z) = .005 \text{ mm/}^\circ\text{C} \quad (6)$$

when allowing a focal adjustment.

### 3. Structure deformation due to 1°C/hr change of ambient air temperature -

If the telescope is built with tubings of identical wall thickness and with the same material, and if the ambient air temperature is uniform surrounding the entire structure, then a change in the ambient air temperature causes a change of the temperature in the metal, but lag behind with a period of time. The surface of the telescope will not suffer from any distortion due to this kind of temperature change ( $\dot{T}$ ), because the entire structure is having a uniform thermal deformation.

It is easy to build a telescope with one kind of material, but it is difficult to maintain the wall thickness of all structural

---

\* This is the result before the telescope was modified on the telescope from a bi-metallic construction to a complete aluminum one.  $\Delta T$  effect on aperture efficiency has not been measured after the modification.

members identical for obvious practical reasons. Hence the rate of temperature change in each member is different from one another at a change of ambient air temperature. It causes a temperature differential within the structure. And the temperature differential within the structure causes distortion of the surface.

The temperature loading  $t_m$  applies to each member in the thermal analysis for the  $\dot{T}$  case. It is expressed as:

$$t_m = \tau \times t \times \dot{T} \quad (7)$$

Where  $\tau$  is the thermal time constant of steel tubings ( $68.9 \times 10^{-3}$  hr/mm) when painted white;  $t$  the wall thickness of tubing and  $\dot{T}$  the time derivative of ambient air temperature. It is intended to maintain the time constant of the entire structure to about 20 minutes. Since the time constant is proportional to the wall thickness, the variation of the wall thickness in the entire structure, except the large suspension members, are limited to 4.8 mm. The analytical results due to the  $T$  effect is listed as follows:

TABLE 2

Influence of  $\dot{T}$  Effect on the Back-up  
Structure With and Without Focal Adjustment  
(see Table 1 for explanation)

	Best fit rms Surface error (mm)	dx	dy	dz	$\phi_x$	$\phi_y$	$\Delta F$
$\dot{T} = 1^\circ\text{C/hr}$	.040	0.	0.	+0.013	0.	0.	Forced to 0
	.008	0.	0.	-.005	0.	0.	.102

Once the  $\dot{T}$  curve is obtained empirically, it can be incorporated to the correction program to make the proper focal adjustments.

Hence the surface error due to the  $\dot{T}$  effect is:

$$\text{rms } (\Delta Z) = .008 \text{ mm-hr/C}^\circ \quad (8)$$

#### 4. Surface error due to temperature effects over a 24 hour period -

The temperature induced surface error is a quadratic sum of error due to temperature difference ( $\Delta T$ ) and time derivative of ambient air temperature ( $\dot{T}$ ). Table 3 listed these separate effects and also its combined results. The error due to  $\Delta T$  is the product of figure 1a and equation (6); and the error due to  $\dot{T}$  the product of figure 1b and equation (8). Table 3 also shows that between 0800 hours and 1900 hours, the surface error due to temperature effect becomes larger and the aperture efficiency might reduce somewhat at the  $\lambda = 1.2$  mm observations.

**TABLE 3** - Surface error due to temperature difference and time derivative of ambient air temperature in a 24-hour period on a typical calm, clear day

hour	$\Delta T(^{\circ}\text{C})$	$\times 5\mu\text{m}/^{\circ}\text{C}$	$T^{\circ}\text{C}/\text{hr} \times 8 \frac{\mu\text{mhr}}{^{\circ}\text{C}}$		thermal surface error ( $\mu\text{m}$ )
18	2.1	11	2.0	16	19
19	2.0	10	1.5	12	16
20	2.0	10	1.1	9	13
21	2.0	10	1.0	8	13
22	2.0	10	1.0	8	13
23	2.0	10	1.0	8	13
24	2.0	10	1.0	8	13
1	2.0	10	1.0	8	13
2	2.0	10	1.0	8	13
3	2.0	10	1.0	8	13
4	2.0	10	1.0	8	13
5	2.0	10	1.0	8	13
6	2.0	10	1.0	8	13
7	2.0	10	1.0	8	13
8	2.0	10	1.2	10	14
9	2.1	11	1.5	12	16
10	2.5	13	2.0	16	21
11	3.0	15	3.5	28	32
12	3.0	15	5.7	46	48
13	3.0	15	5.7	46	48
14	3.0	15	4.3	34	37
15	3.0	15	2.1	17	23
16	3.0	15	1.2	10	18
17	2.6	13	1.4	11	17

$$\text{rms}(\text{error}) = 22 \mu\text{m}$$

## POINTING ERROR DUE TO TEMPERATURE EFFECT

Without a very clear picture of temperature difference distribution on the back-up structure, it is probably safe to assume a peak pointing error will arrive when the temperature gradient across the aperture becomes pronounced. For example, this situation will arise when the telescope points to horizon for a long period of time, the vertical temperature difference in the ambient air will produce a temperature difference at different parts of the structure across the aperture, as well as across the feed support legs. The detailed analysis of this case on the back-up structure as well as a detailed model of the feed leg structure produced the following results:

Lateral shift of the main reflect	$\Delta m = -.022 \text{ mm/C}^\circ$	
Rotation of the main reflector	$\alpha_m = -9 \times 10^{-7} \text{ rad/C}^\circ = -.19 \text{ sec/C}^\circ$	
Lateral shift of the subreflector	$\Delta s = +.056 \text{ mm/C}^\circ$	
Rotation of the subreflector	$\alpha_s = +1.7 \text{ sec/C}^\circ$	(9)
Lateral displacement of Casse- grain Receiver	$\Delta P = 0$	

With reference to the detail description of pointing error combination described in the appendix. The thermal pointing error is:

$$\text{Thermal pointing} \left\{ \begin{array}{l} = 0.68 \text{ sec/C}^\circ \text{ peak} \\ = 0.47 \text{ sec/C}^\circ \text{ rms} \\ = 1.5 \text{ sec} \text{ day } (\Delta T=3^\circ\text{C}) \\ = 1.0 \text{ sec} \text{ night } (\Delta T=2^\circ\text{C}) \end{array} \right. \quad (10)$$

THE GRAVITY DEFORMATION OF THE BACK-UP STRUCTURE

The theory of homology optimization is described in great length in various reports and papers. Based on the derivation of the optimization procedure, a special computer program was written for this purpose. A structural design with an optimum solution was eventually resolved.

The structural design should be a realistic one, adding constraints in the process of optimization. These constraints included the requirements that all bar areas are having positive cross-sections, that all members are structurally stable and that the cross-sectional areas of some members remain unchanged.

The homology program optimizes the solution by yielding a new set of cross-sectional areas for members, with the geometry of the structure remaining unchanged. Hence realistic geometry must be the first concern prior to optimization. For example, no physical interference are allowed, and no two members are connected with an angle smaller than 15°.

A structural design of the 25-m diameter telescope capable of observing mm wavelength has finished. The structure now has a 4 m x 4 m vertex room, capable of having four receivers weighing 450 kg each installed as a cluster.

The homologous solution is listed in detail in Table 4.

TABLE 4  
Homologous Solution  
(See Table 1 for explanation)

Loading	Best fit rms Surface error (mm)	dx	dy	dz	$\phi_x$	$\phi_y$	$\Delta F$
Gravity= -Z	.001	0.	0.	-4.62	0.	0.	+1.74
Gravity= +Y	.002	0.	6.76	0.	$-3.6 \times 10^{-4}$	0.	0.

The solution in table 4 is purely a mathematical one. In reality some further consideration must be taken into account. The first consideration is to replace each structural member with a cross-section which is readily available in steel industries. A computer program called REPLACE is written, with catalogue of steel tubings collected from the industry stored permanently in the disc file. This program can search the closest cross-sectional bar area, checked again with more detail concerns in design: the weldability, local buckling, maintain the thermal time constant of the entire structure and stress analysis according to the specification of American Institute of Steel construction. The fatigue due to wind excited vibration was not considered, since the telescope is to operate with the dome in closed position in a windy situation. The surface degraded somewhat after this operation, and the detailed result is listed in Table 5.

TABLE 5  
Replacement of Commercially Available Tubings  
(See Table 1 for explanation)

Loading	Best fit rms Surface error (mm)	dx	dy	dz	$\phi x$	$\phi y$	$\Delta F$
Gravity= -Z	.009	0.	0.	-4.62	0.	0.	+1.73
Gravity= +Y	.002	0.	6.76	0.	$-3.6 \times 10^{-4}$	0.	0.

Error in construction is a very complicated matter. Two types of errors are presently taken into account. The first is the misalignment of members causing the locations of joints different from what are called for in the design. The construction specification of similar structures would allow up to  $\pm 6$  mm due to misalignment. The second type of error is the difference of cross-sectional areas between an actual member used and those stated in the catalogs from the steel industry. The industry had claimed that a 3% deviation of cross-sectional area should be accounted for.

Additional analysis of the back-up structure, with joint locations randomly shifted by 6 mm, and cross-sectional area changed by 3% has been made. The surface accuracy is further degraded, with the results shown in Table 6.

TABLE 6  
Construction Errors: Joint Misalignments  
and Deviation of Cross-Sectional Areas  
(see Table 1 for explanation)

Loading	Best fit rms Surface error (mm)	dx	dy	dz	$\phi_x$	$\phi_y$	$\Delta F$
Gravity= -Z	.015	0.	0.	-4.62	0.	0.	+1.70
Gravity= +Y	.011	0.	6.80	0.	$-3.6 \times 10^{-4}$	0.	0.

The analysis was carried one more step forward, in order to find out the effects of slight increases of weight and slight decreases of stiffness due to the construction of joints. We have so far not spent any effort to develop the design of the joints. Knowledge from the 65-m study showed that the average weight increase would be 2.5%, and the average stiffness decrease 3%.

TABLE 7

Surface Deviation Due to Additional Increase  
of Weight and Decrease of Stiffness  
(see Table 1 for explanation)

Loading	Best fit rms Surface error (mm)	dx	dy	dz	$\phi_x$	$\phi_y$	$\Delta F$
Gravity= -Z	.017	0.	0.	-4.7	0.	0.	+1.72
Gravity= +Y	.012	0.	6.84	0.	$-3.7 \times 10^{-4}$	0.	0.

Figure 3 shows the surface error over the range from zenith angle of  $0^\circ$  to  $90^\circ$ , with surface plates adjusted at  $45^\circ$  (arbitrarily chosen).

#### FUTURE WORK

Presently, due to the limitation of the homology optimization program, the structure considered can have a maximum of 72 nodes, and 283 connections. The program can be expanded to handle 160 nodes, and 1300 connections by expanding the program to the full capacity of the present NRAO computer (IBM 360/65). There is no urgent need to do so; however, it is a handy tool to have.

The intermediate structures, which bridge across the homologous points and support the surface plates, are presently represented by spring constants between the homologous points during the optimization. We are in the process of replacing these spring constants with the models of intermediate panels with the general purpose structural analysis program (NASTRAN, STRUDL) with all panel structures and the back-up structure coupled together. Accuracy of the surface of this complicated model would render a good check of our previous results.

We are about to start the engineering drawings of the reflector. This will be limited to mostly control drawings instead of details.

## APPENDIX 1

### Pointing Error of Cassagrain System for the 25-m

The pointing error of a Cassegrain System is a combination of beam tilting caused by

- 1) Lateral shift of the best fit paraboloid  $\Delta_m$ , the tilt of beam is

$$\theta_{\Delta_m} = -(BDF) \frac{\Delta_m}{f_m} \quad (1)$$

- 2) Rotation of the best fit paraboloid  $\alpha_m$ , the tilt of beam is

$$\theta_{\alpha_m} = + (1+BDF) \alpha_m \quad (2)$$

- 3) Lateral shift of the subreflector  $\Delta_s$ , causing the tilt of beam,

$$\theta_{\Delta_s} = +(BDF) \frac{\Delta_s}{f_m} \left(1 - \frac{f_s}{L}\right) \quad (3)$$

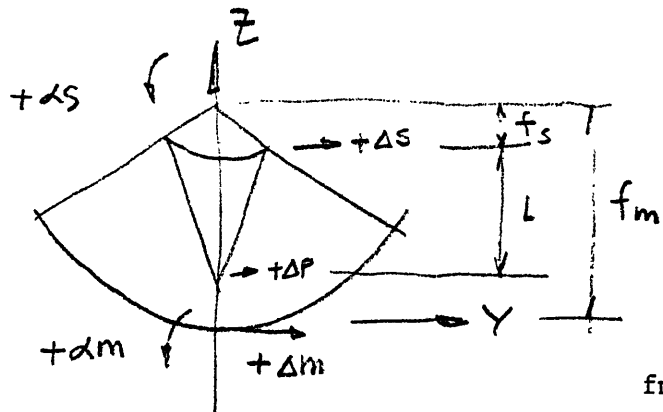
- 4) Rotation of the subreflector  $\alpha_s$  causing a tilt of the beam

$$\theta_{\alpha_s} = -2 \times BDF \times \alpha_s \times \frac{f_s}{f_m} \quad (4)$$

- 5) Lateral displacement of the Cassegrain receiver and its corresponding tilt of beam,

$$\theta_{\Delta_p} = -BDF \frac{\Delta_p}{L} \frac{f_s}{f_m} \quad (5)$$

The geometry and the sign convention are shown in the following figure:



$$\begin{aligned}
 f_m &= 10,500 \text{ mm} \\
 f_s &= 589.3 \text{ mm} \\
 L &= 9,310.7 \text{ mm} \\
 \text{BDF} &= 0.8
 \end{aligned}$$

With the given geometry and equation (1) through (4), the combined tilt of beam is as follows, with displacement in mm and sev.

$$\begin{aligned}
 \theta_T &= \theta_{\Delta m} + \theta_{\alpha m} + \theta_{\alpha s} + \theta_{\Delta P} + \theta_{\Delta S} \\
 &= -15.695 (\Delta m) + 1.8 (\alpha m) + 14.702 (\Delta S) - 0.09 (\alpha S) - 0.993 (\Delta P)
 \end{aligned}$$

APPENDIX 2

Weight of the Elevation Structure

	<u>Kg</u>
Feed Leg Structure	997
Surface plates and attachments	10,062
Intermediate panels	17,667
Backup structure	29,264
Subreflector or Receiver at apex of feed leg structure	906
Vertex room with four receivers	4,530
Counter Weight	11,370

---

Weight on elevation bearings = 74,796

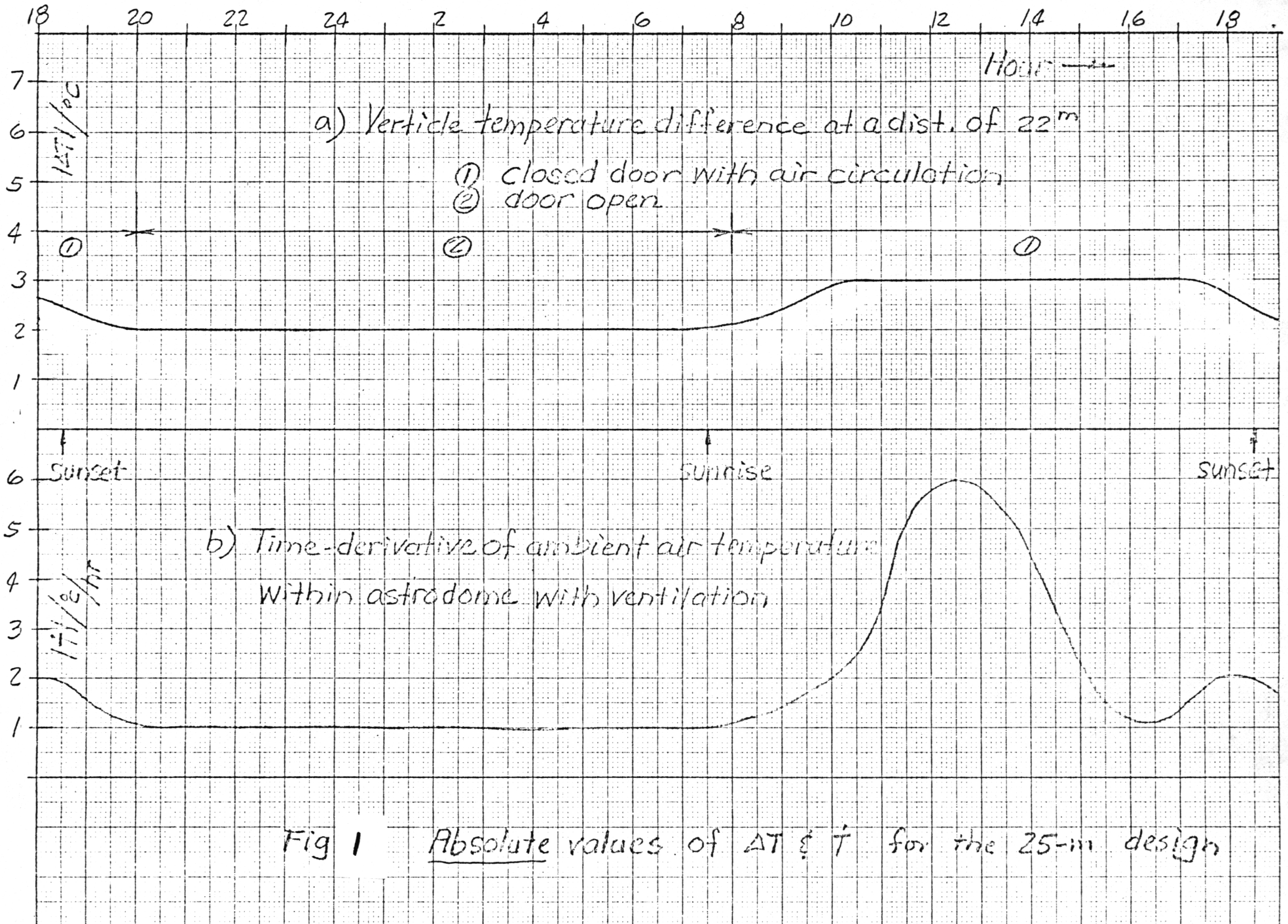


Fig 1 Absolute values of  $\Delta T$  &  $\dot{T}$  for the 25-m design

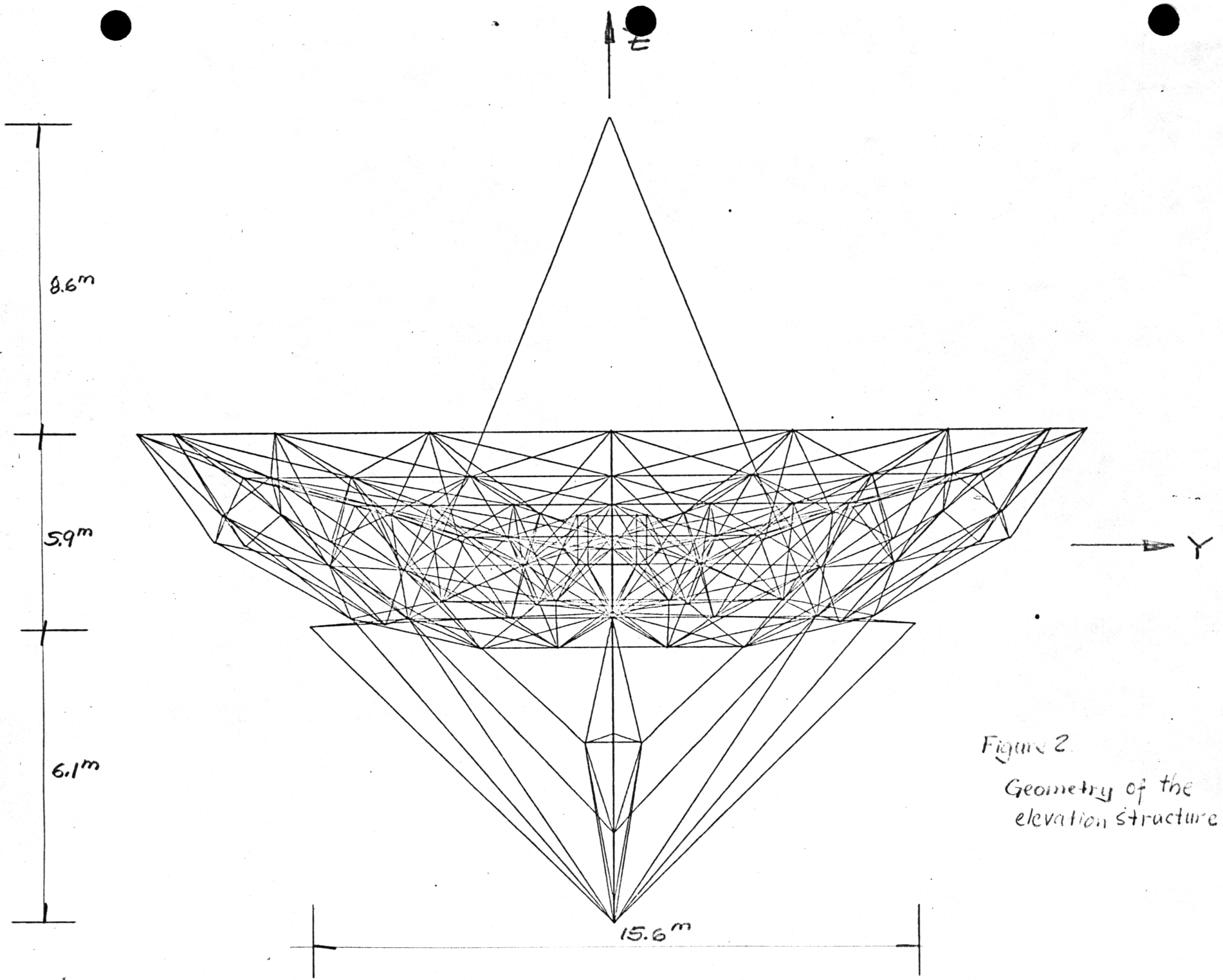
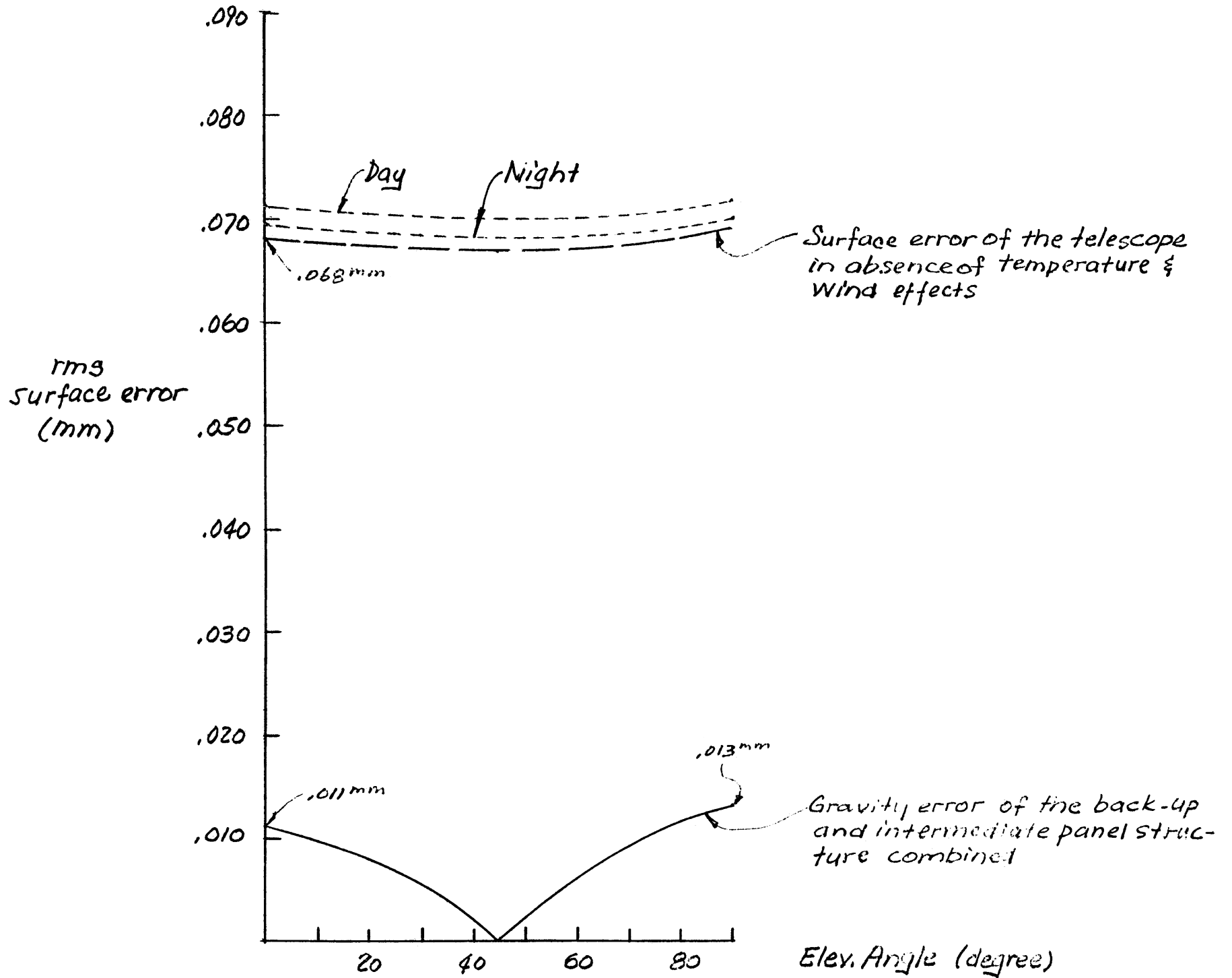


Figure 2  
Geometry of the  
elevation structure

Figure 3. Predicted surface error of the 25-m



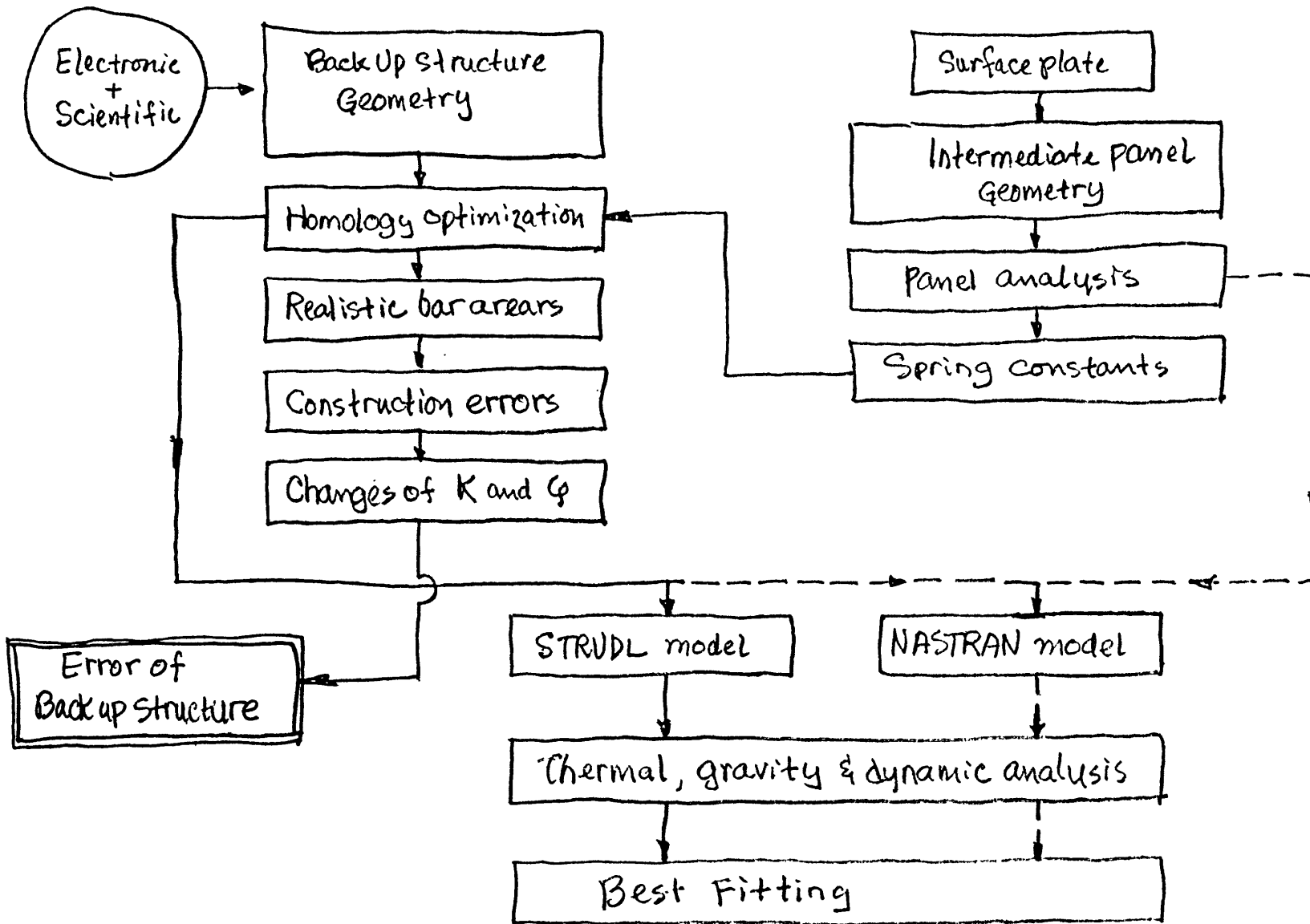


Figure 4. Work schedule for the back-up structure design

- Works done up to date
- - - Future work

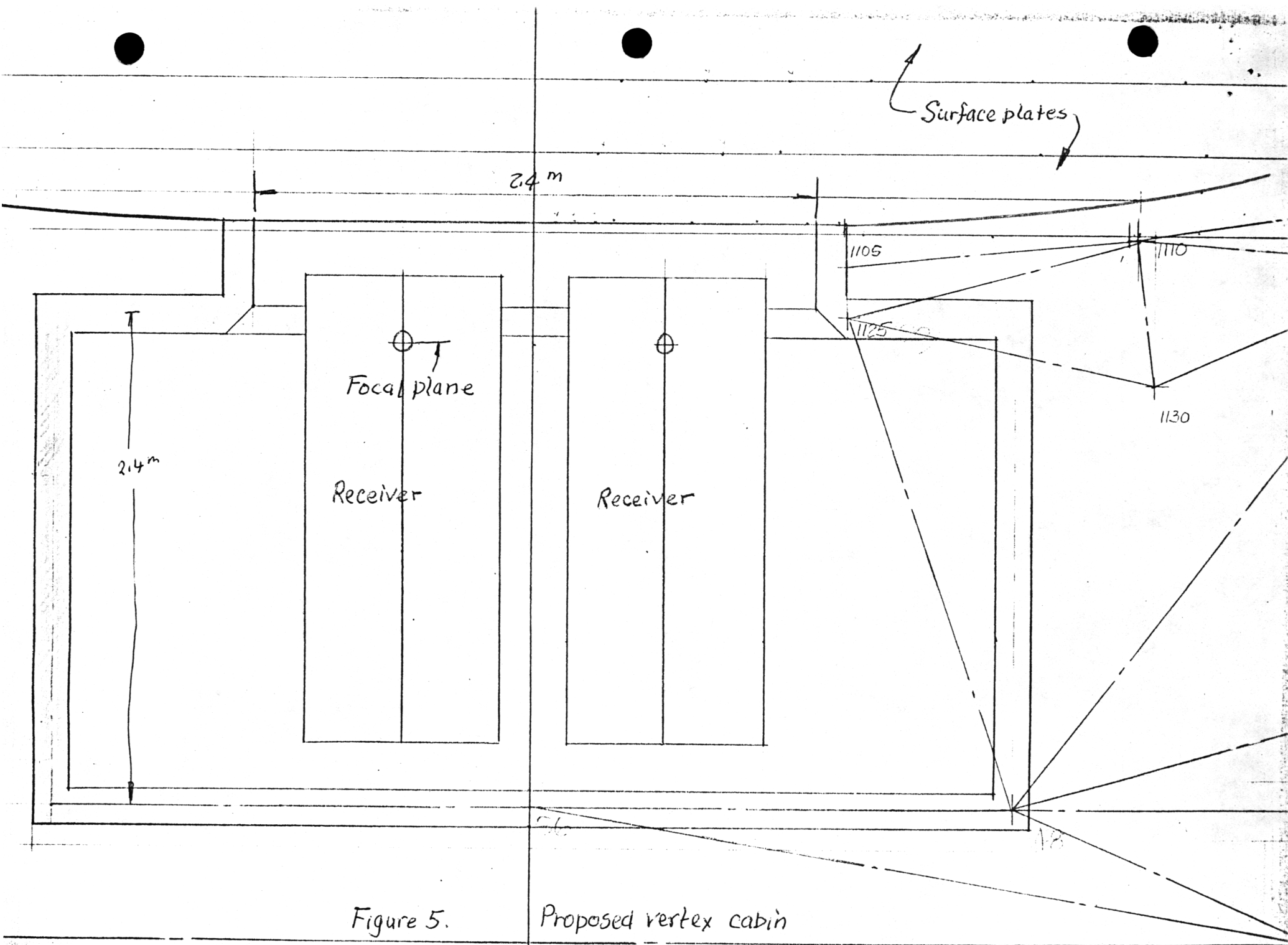


Figure 5. Proposed vertex cabin